Biomass-Derived Potassium-Doped Reduced Graphene Oxide-like Material for High-Performance Supercapacitors: Experimental and Computational Analysis

Chetna Tewari[a], Kundan Singh Rawat[a,b], Diksha Bhatt[b], Boddepalli SanthiBhushan[c], Young Nam Kim[a], Somi Yoon[a,d], Anurag Srivastava[e], Jun-Wei Zha[f], Nanda Gopal Sahoo[c], Yong Chae Jung[a,*]

[a] *RAMP Convergence Research Center, Korea Institute of Science and Technology (KIST), 92 Chudong-ro, Bongdong-eup, Wanju-gun, Jeonbuk, 55324, Republic of Korea.*

[b] *Prof. Rajendra Singh Nanoscience and Nanotechnology Centre, Department of Chemistry D.S.B. Campus, Kumaun University Nainital, Uttarakhand, India.*

[c] *Department of Electronics and Communications Engineering, Indian Institute of Information Technology, Allahabad, UP-211015*

[d] *Department of Organic and Nano Engineering, Hanyang University, 222 Wangsimni-ro, Seongdong-gu, Seoul 04763, Republic of Korea*

[e] *Department of Engineering Sciences, ABV – Indian Institute of Information Technology and Management, Gwalior, M.P. – 474015*

[f] *State Key Laboratory of Alternate Electrical Power System with Renewable Energy Sources, School of Electrical and Electronic Engineering, North China Electric Power University, Beijing 102206, China*

** Corresponding authors emails: ycjung@kist.re.kr (Yong Chae Jung)*

Contents

Supporting Table

Table S1: Comparison of PrGO (this work) with previously reported waste and biomass-derived carbon materials for supercapacitor applications.

Electrode Material	Heteroatom Content	Specific Capacitance	Electrolyte	Ref.
Waste tea-derived AC	O: 3.34% P: 0.48%	89.3 F/g @ 1 A/g (KOH) 73.8 F/g @ 1 A/g (H_2SO_4)	KOH, H_2SO_4	[1]
Chestnut shells derived AC (NaOH activated)	C: 68.89 % O: 24.44 %	125 F/g @ 2.5 A/g	1 M H_2SO_4	[2]
Pumpkin skin derived graphic-like carbon	-	274 F/g @ 1.0 A/g	1 M KOH	[3]
Waste tea-derived AC doped with S	O: 6.57% P: 0.44% S: 4.94%	144.7 F/g @ 1 A/g (KOH) 101.9 F/g @ 1 A/g (H_2SO_4)	KOH, H_2SO_4	[1]
Waste hemp fibers (KOH activated)	–	122 F/g @ 5 mV/s	1 M H_2SO_4	[4]
Poly(m-phenylene isophthalamide)-derived AC	–	175 F/g @ 5 mV/s	5.25 M H_2SO_4	[5]
Lignin-derived AC	–	102.3 F/g @ 1 mV/s	6 M KOH	[6]
Sugarcane bagasse (NaOH activated)	–	141 F/g @ 0.5 A/g	6 M KOH	[7]
Milk powder-derived carbon (KOH activated)	N: 0.77% O: 1.10%	304 F/g @ 0.2 A/g	1 M Li_2SO_4	[8]
Aniline & pyrrole-derived hollow nanospheres	N: 2.55%	180 F/g @ 1 A/g; 201 F/g @ 5 mV/s	6 M KOH	[9]

Fish skin-derived porous carbon (KOH used)	N: 8.18% O: 14.02% S: 2.25%	282 F/g @ 1 A/g	6 M KOH	[10]
Human hair-derived carbon flakes (KOH activated)	N: 4.38% O: 5.39% S: 1.51%	126 F/g @ 1 A/g	1 M $LiPF_6$ in EC/DEC	[11]
Willow catkin-derived N, S co-doped nanosheets	N: 4.62% O: 12.17% S: 2.56%	298 F/g @ 0.5 A/g	1 M Na_2SO_4	[12]
Banana stem-derived hard carbon (KOH activated)	–	118 F/g @ 0.5 mV/s	6 M KOH	[13]
Banana stem-derived hard carbon (H_3PO_4 activated)	–	202.11 F/g @ 2 mV/s	6 M KOH	[13]
Corn-cob-derived hard carbon	–	309.81 F/g @ 2 mV/s	6 M KOH	[13]
Potato starch-derived hard carbon	–	99.9 F/g @ 2 mV/s	6 M KOH	[13]
Rice husk-derived AC (KOH activated)	O: 7.06% K: 1.59% Si: 0.26%	143 F/g @ 5 mV/s	6 M KOH	[114]
Waste plastic derived rGO	-	185.12 F/g @ 5 mV/s	1 M H_2SO_4	[15]
Waste plastic derived rGO nanocomposite with Fe3o4	-	326.87 F/g @ 5 mV/s	1 M H_2SO_4	[15]
Quercus ilex leaves derived metal doped graphene	Ca: 3.17 % K: 6.15% Mg: 2.36%	18.2 F/g @ 5 mV/s	PVA–H_3PO_4	[16]
Tire waste-derived graphene (nanocatalyst and ZnO used)	C: 95.66% O: 2.75% Zn: 1.59%	316 F/g @ 5 mV/s	1 M H_2SO_4	[17]
N/B-doped graphene from polyamic acid	C: 89.70% O: 5.79% N: 1.73% B: 2.77%	40.4 mF/cm² @ 0.05 mA/cm²	PVA–H_2SO_4 gel	[18]
N/P co-doped graphene	P: 0.57–1.57%	244 F/g @ 0.1 A/g	6 M KOH	[19]

N & P dual-doped graphene from waste plastics	C: 79.67% O: 13.57% P: 2.18% N: 4.58%	283.08 F/g @ 2 mV/s	1 M H_2SO_4	[20]
Oil palm shell-derived AC	–	156 F/g @ 2 mV/s	1 M H_2SO_4	[21]
Oil palm shell-derived AC/NiO composite	C: 36 wt% O: 23.3 wt% Ni: 36.2 wt% P: 4.5 wt%	288 F/g @ 2 mV/s	1 M H_2SO_4	[21]
Commercial AC	-	94 F g^{-1} @ 0.2A/g	1 M Na_2SO_4	[22]
rGO	-	**81.2 @10 mVs^{-1}**	6M KOH	[23]
GO	-	**166.4** @ 10 mV/s	6M KOH	[23]
Graphene nanoribbons	-	**14.1** @ 10 mV/s	6M KOH	[23]
rGO	C: 82 wt%, O: 15.69 wt% N: 2.31 wt%	**110 @** 0.5A/g	$LiPF_{6\ in}$ ethylene carbonate and diethylene carbonate (1:1 *v*/*v*)	[24]
CNTs	-	**15 @** 0.5A/g	$LiPF_{6\ in}$ ethylene carbonate and diethylene carbonate (1:1 *v*/*v*)	[24]
PrGO (no activation agent or catalyst used)	C: 88.41% O: 9.05% K: 2.15%	**302.08 F/g @ 2 mV/s**	1 M H_2SO_4	**This work**

Table S2: Capacitance and power density of PrGO with literature under the same electrolyte and testing conditions.

S.N.	Electrode Material	Specific Capacitance	Energy Density (Wh/Kg)	Electrolyte	Ref.
1.	Tea-derived AC	73.8 F/g @ 1 A/g	6.56	1 M H_2SO_4	[1]
2.	S-Doped AC	101.9 F/g @ 1 A/g	9.06	1 M H_2SO_4	[1]
3.	Chitin derived N & P doped porous carbon	227 F/g @ 0.5 A/g	7.9	1 M H_2SO_4	[25]
4.	Jack wood biochar	147 F/g @ 2 mV s−1	7.30 at 1.0**mA cm^{-2}**	1 M H_2SO_4	[26]
5.	Activated carbon	175.19 F/g @ 1 A/g	6.08	1M H_2SO_4	[27]
6.	Self-assembled Graphene Hydrogels	87.6 F/g @ 1 A/g	5.1	1 M H_2SO_4	[28]
7.	Graphene Hydrogel	186 F/g @ 1A/g	0.61	1 M H_2SO_4	[29]
8.	Graphene foam/PVA	65 F/g @ 0.2 A/g	12	1 M Na_2SO_4	[30]
9.	Hierarchical porous carbon	48.7 F/g @ 0.2A/g	6.77	6 M KOH/PVA	[31]
10.	Agarose-Bound Activated Carbons	30.0 F/g @ 0.5A/g	13.5	1 M H_2SO_4	[32]
11.	Commercial activated carbon (AC)	94 F/g @ 0.2A/g	13	1 M Na_2SO_4	[22]
12.	AC	24 F/g @ 1000	11	1 M-NaNO3–	[33]

		mA/g		Ethylene glycol	
13.	YF-50	30 F/g @ 1 A/g	3.86 @1.0 V	1 M H_2SO_4	[34]
14.	Aloe-Vera derived Carbon	73 F/g @ 1 A/g	14.7 @1.2 V	1 M H_2SO_4	[35]
15.	CLCF	50 F/g @ 1 A/g	6.9 @1.0 V	1 M H_2SO_4	[36]
16.	MMPGC	105 F/g @ 4 mV s−1	4	2 M H_2SO_4	[37]
17.	PrGO	98 F/g @ 0.2 A/g	11	1 M H_2SO_4	This work.

Table S3. Comparison of equivalent series resistance (ESR) values of the present persimmon-derived reduced graphene oxide-like electrode with previously reported state-of-the-art carbon-based supercapacitor electrodes under different operating voltages and electrolyte systems.

S.No.	Electrode /Device Material	Operating voltage	Electrolyte	ESR (Ω)	Reference
1	Biomass-derived N-doped porous carbon	–1.0 - 0 V	6M KOH	0.83-1.3	[38]
2	Activated carbonaceous polypyrrole nanotubes	–1.0 - 0 V	6M KOH and 1M H_2SO_4	0.85-1.5	[39]
3	porous carbon electrode with polyaniline	0 - 0.8V	1 M H_2SO_4	1.2-2.2	[40]
4.	Automobile soots	0 - 1.2V	1 M Na_2SO_4	1.5	[41]
5	Activated Carbon of Glucose with Potassium Nitrate	0 - 2.5V	1 M TEABF4/PC	2.5	[42]
6	activated carbon derived from asparagus waste	0 - 2.5 V	Gel polymer electrolyte	4-7	[43]
7.	LLDPE derived graphene	0 – 1.2V	1 M H_2SO_4	0.71-0.79	[44]
8.	Waste plastic into	0 – 1V	1 M H_2SO_4,	0.92-	[45]

	reduced graphene oxide		2MKCL, 6M KOH	2.86	
9.	WT-rGO@NiCoFe-LDH composites	0 – 0.6 V	2M KOH	0.85	[46]
10.	WT-rGO@MoS2 composites	0 – 0.9	1M H_2SO_4	0.92	[47]
11.	Persimmon derived-reduced graphene oxide like material	0 – 0.9V	1 M H_2SO_4	0.65	**This Work**

Supporting Figures

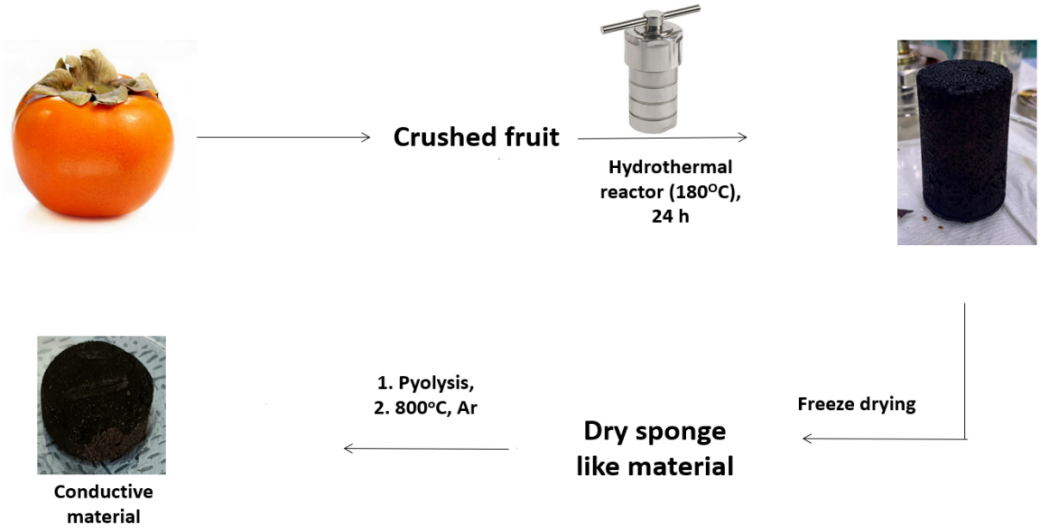

Fig. S1. Method for synthesis of rGO from persimmon fruit.

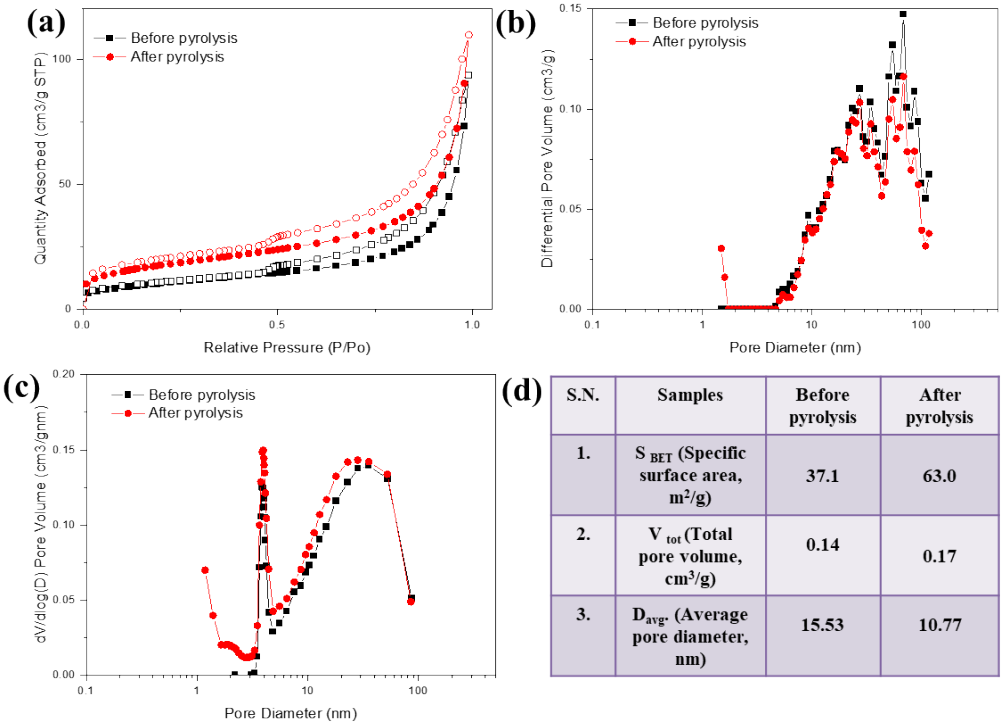

(d)

S.N.	Samples	Before pyrolysis	After pyrolysis
1.	S_{BET} (Specific surface area, m^2/g)	37.1	63.0
2.	V_{tot} (Total pore volume, cm^3/g)	0.14	0.17
3.	$D_{avg.}$ (Average pore diameter, nm)	15.53	10.77

Fig. S2. (a) N_2 adsorption–desorption isotherms at 77 K before and after pyrolysis; (b) BJH pore size distribution (adsorption branch); (c) differential pore volume (desorption branch); and (d) corresponding textural parameters.

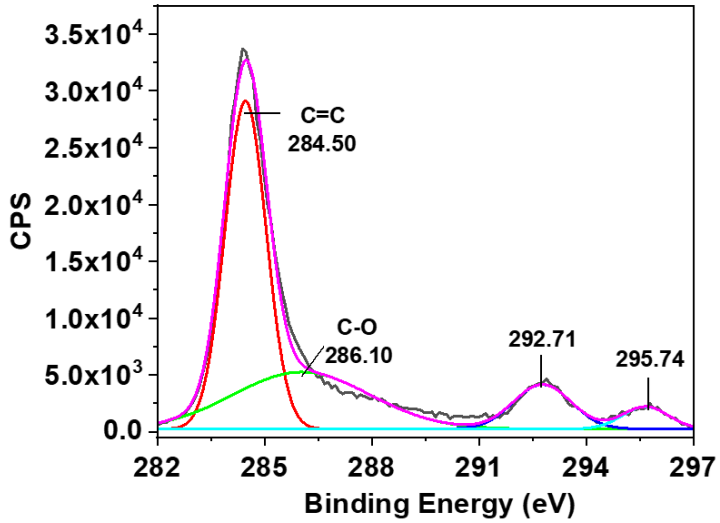

Fig. S3. XPS spectra showing the binding energy of carbon in PrGO.

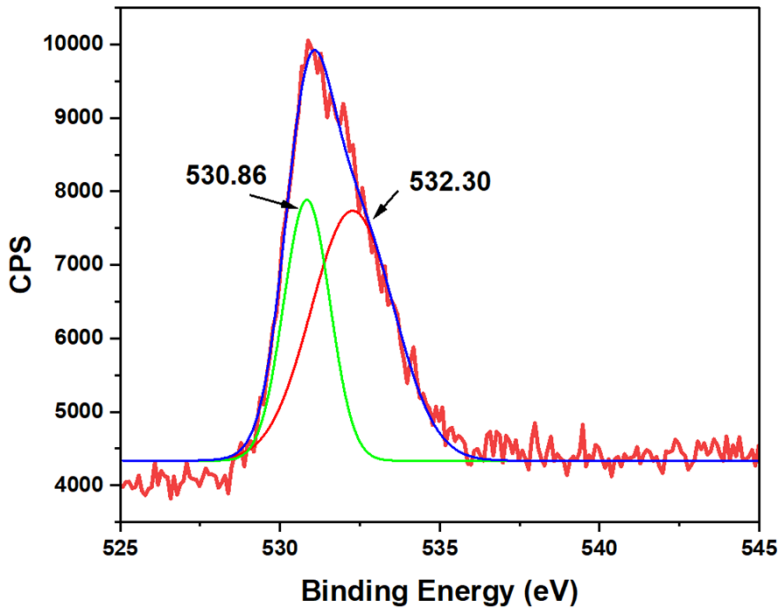

Fig. S4. XPS spectra showing the binding energy of oxygen in PrGO.

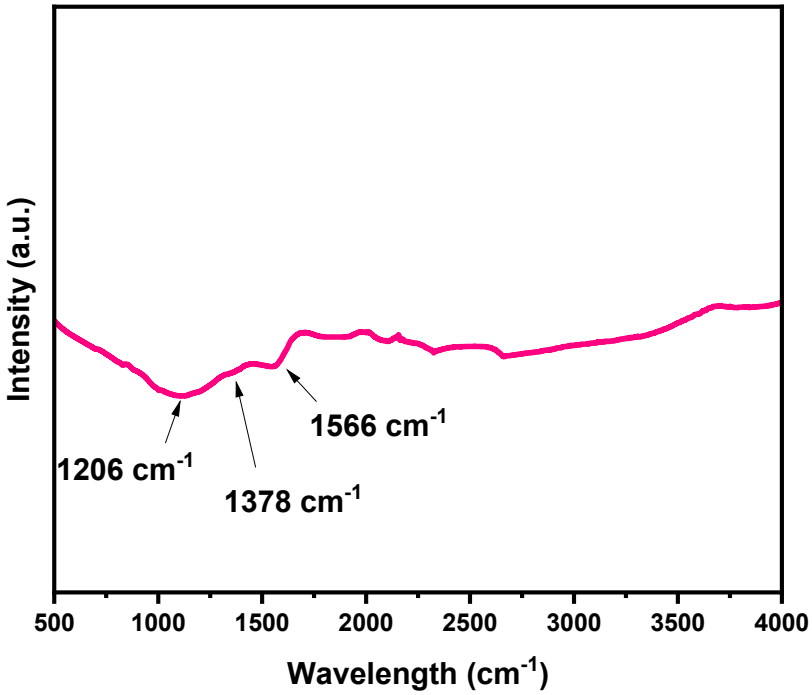

Fig. S5. FTIR spectra of PrGO.

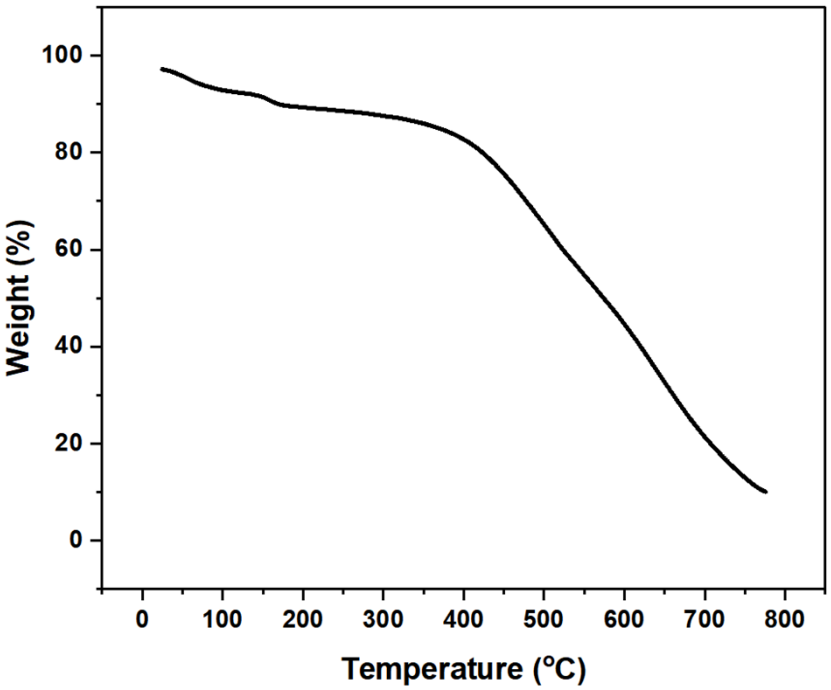

Fig. S6. TGA analysis of PrGO.

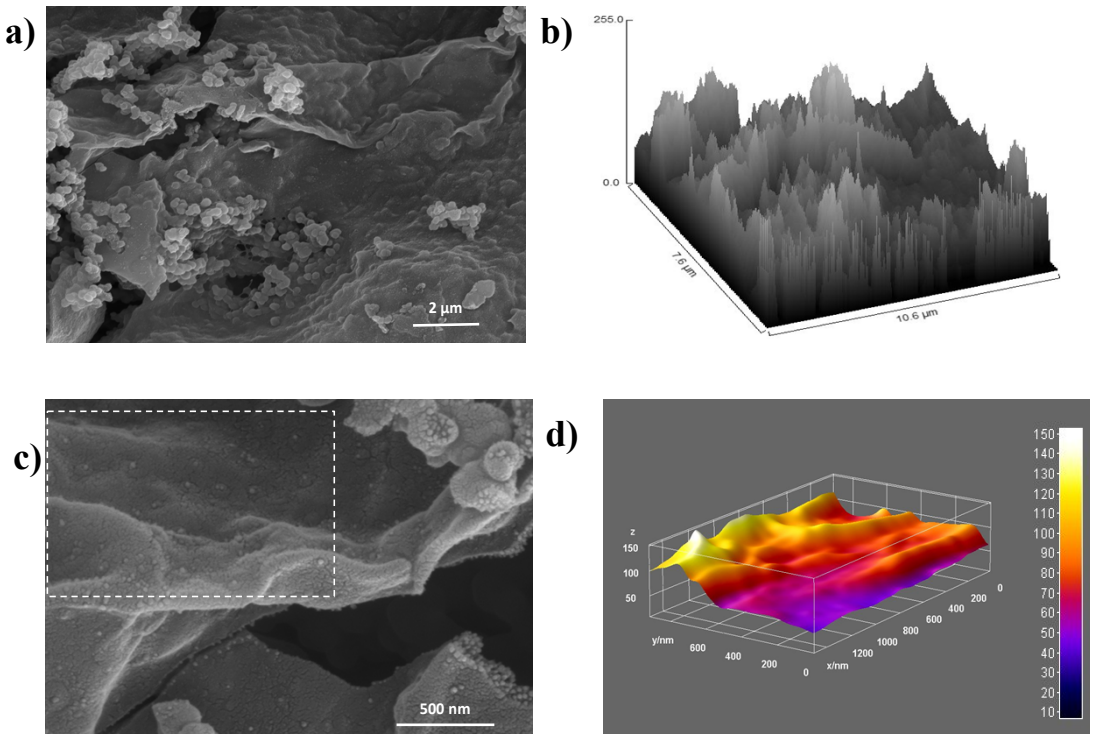

Fig. S7. (a) SEM image of the prepared PrGO, (b) hill stack view illustrating surface roughness, (c) SEM image at 500 nm magnification, and (d) 3D surface plot generated from the highlighted area in (c).

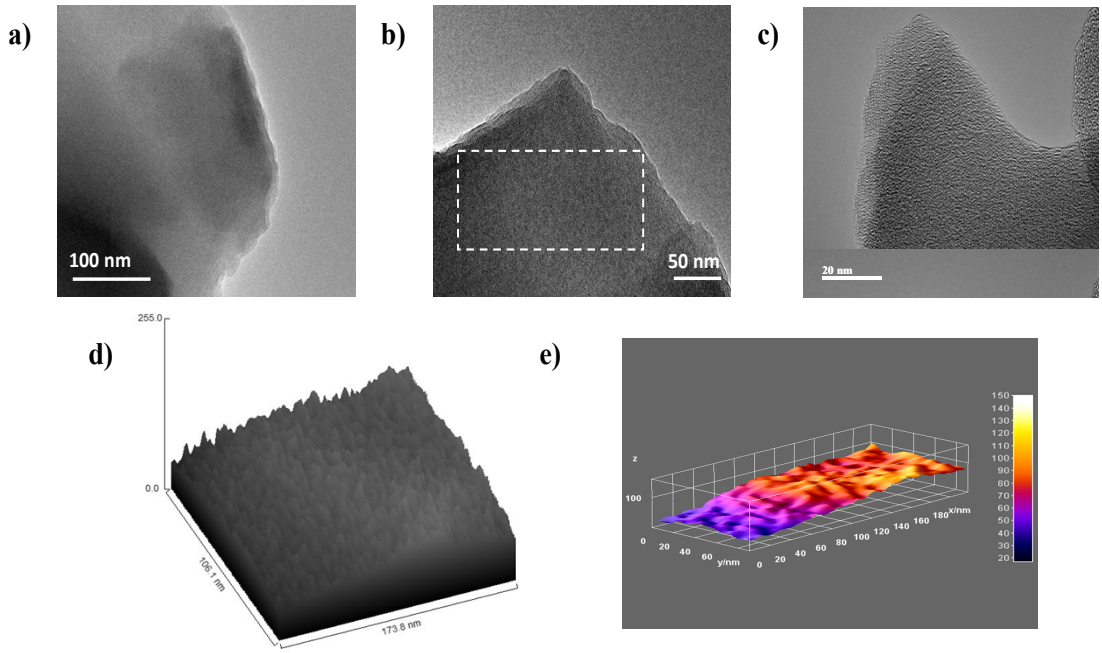

Fig. S8. (a-c) HR-TEM images of the prepared PrGO; (d) hill stack view illustrating surface roughness, generated from the highlighted region in (b); (e) 3D surface plot generated from the highlighted area in (b).

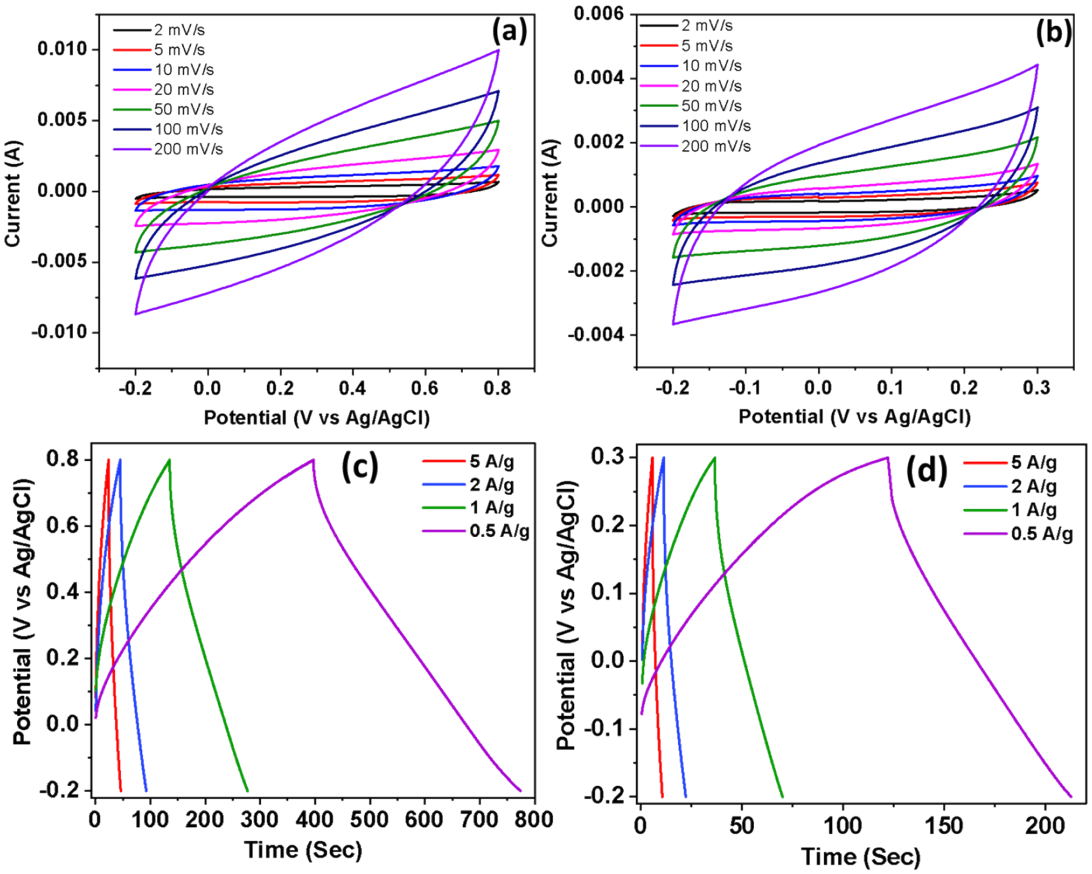

Fig. S9. (a) CV curves at various scan rates in 2 M KCl, (b) CV curves at various scan rates in 6 M KOH, (c) GCD curves at different current densities in 2 M KCl, and (d) GCD curves at different current densities in 6 M KOH.

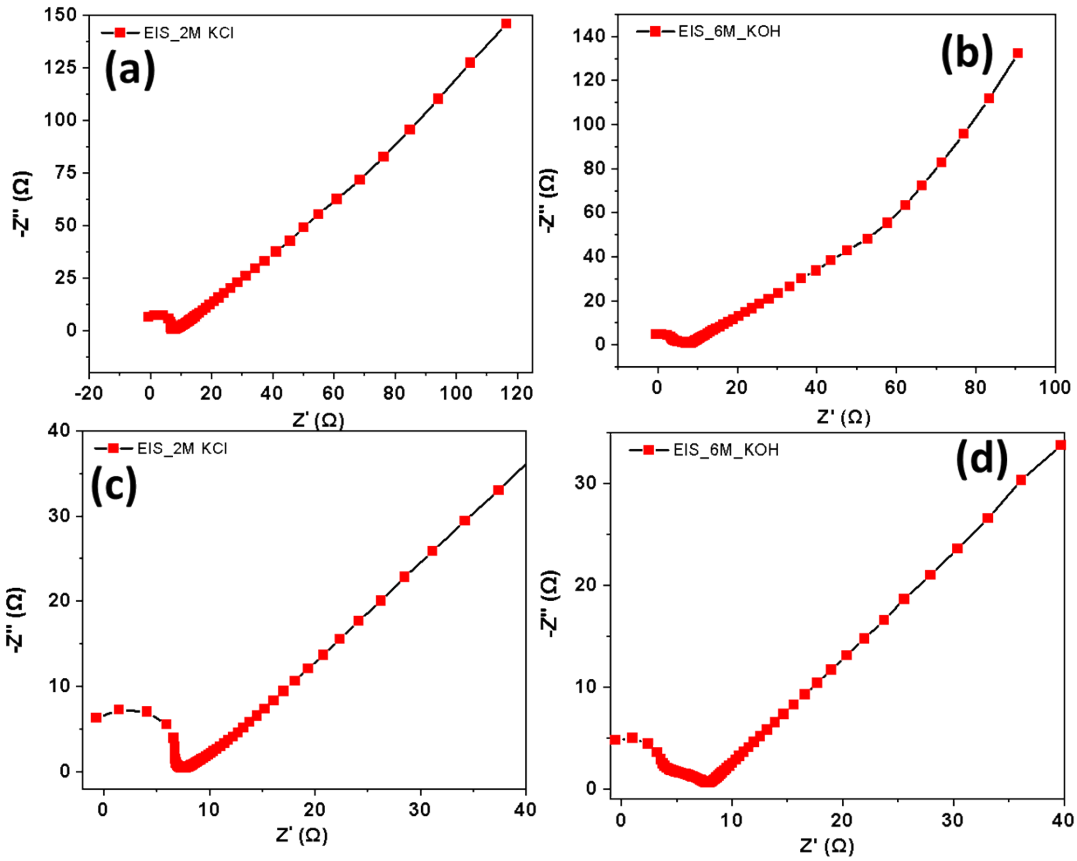

Fig S10. a) Nyquist plot in 2 M KCl, (b) Nyquist plot in 6 M KOH, (c) magnified view of the Nyquist plot in 2 M KCl, and (d) magnified view of the Nyquist plot in 6 M KOH.

Supporting References

References:

1. Yaglikci, S., Gokce, Y., Yagmur, E. and Aktas, Z., 2020. The performance of sulphur doped activated carbon supercapacitors prepared from waste tea. *Environmental Technology*, *41*(1), pp.36-48. https://doi.org/10.1080/09593330.2019.1575480.
2. Genel, İ., Yardım, Y. and Saka, C., 2025. Green synthesis of hierarchical nitrogen-doped porous activated carbon material based on biomass waste for high-performance energy storage as supercapacitor. *Biomass and Bioenergy*, *197*, p.107818. https://doi.org/10.1016/j.biombioe.2025.107818.
3. Guye, M.E., Dabaro, M.D. and Kim, H., 2025. Biomass-derived graphitic-like hierarchical porous carbon for electrochemical supercapacitor application. *Journal of Energy Storage*, *115*, p.116037. https://doi.org/10.1016/j.est.2025.116037.
4. Mijailović, D.M., Vukčević, M.M., Stević, Z.M., Kalijadis, A.M., Stojanović, D.B., Panić, V.V. and Uskoković, P.S., 2017. Supercapacitive performances of activated highly microporous natural carbon macrofibers. *Journal of The Electrochemical Society*, *164*(6), p.A1061. 10.1149/2.0581706jes.
5. Leitner, K., Lerf, A., Winter, M., Besenhard, J.O., Villar-Rodil, S., Suarez-Garcia, F., Martinez-Alonso, A. and Tascón, J.M.D., 2006. Nomex-derived activated carbon fibers as electrode materials in carbon based supercapacitors. *Journal of power sources*, *153*(2), pp.419-423. https://doi.org/10.1016/j.jpowsour.2005.05.078.
6. Saha, D., Li, Y., Bi, Z., Chen, J., Keum, J.K., Hensley, D.K., Grappe, H.A., Meyer III, H.M., Dai, S., Paranthaman, M.P. and Naskar, A.K., 2014. Studies on supercapacitor electrode material from activated lignin-derived mesoporous carbon. *Langmuir*, *30*(3), pp.900-910. https://doi.org/10.1021/la404112m.
7. Hao, P., Zhao, Z., Tian, J., Li, H., Sang, Y., Yu, G., Cai, H., Liu, H., Wong, C.P. and Umar, A., 2014. Hierarchical porous carbon aerogel derived from bagasse for high performance supercapacitor electrode. *Nanoscale*, *6*(20), pp.12120-12129. https://doi.org/10.1039/C4NR03574G.
8. Pokrzywinski, J., Keum, J.K., Ruther, R.E., Self, E.C., Chi, M., Meyer III, H., Littrell, K.C., Aulakh, D., Marble, S., Ding, J. and Wriedt, M., 2017. Unrivaled

combination of surface area and pore volume in micelle-templated carbon for supercapacitor energy storage. *Journal of Materials Chemistry A*, *5*(26), pp.13511-13525. 10.1039/C7TA03655H.

9. Xu, F., Tang, Z., Huang, S., Chen, L., Liang, Y., Mai, W., Zhong, H., Fu, R. and Wu, D., 2015. Facile synthesis of ultrahigh-surface-area hollow carbon nanospheres for enhanced adsorption and energy storage. *Nature communications*, *6*(1), p.7221. https://doi.org/10.1038/ncomms8221.
10. Niu, J., Liu, M., Xu, F., Zhang, Z., Dou, M. and Wang, F., 2018. Synchronously boosting gravimetric and volumetric performance: Biomass-derived ternary-doped microporous carbon nanosheet electrodes for supercapacitors. *Carbon*, *140*, pp.664-672. https://doi.org/10.1016/j.carbon.2018.08.036.
11. Qian, W., Sun, F., Xu, Y., Qiu, L., Liu, C., Wang, S. and Yan, F., 2014. Human hair-derived carbon flakes for electrochemical supercapacitors. *Energy & Environmental Science*, *7*(1), pp.379-386. https://doi.org/10.1039/C3EE43111H.
12. Li, Y., Wang, G., Wei, T., Fan, Z. and Yan, P., 2016. Nitrogen and sulfur co-doped porous carbon nanosheets derived from willow catkin for supercapacitors. *Nano energy*, *19*, pp.165-175. https://doi.org/10.1016/j.nanoen.2015.10.038.
13. Ghosh, S., Santhosh, R., Jeniffer, S., Raghavan, V., Jacob, G., Nanaji, K., Kollu, P., Jeong, S.K. and Grace, A.N., 2019. Natural biomass derived hard carbon and activated carbons as electrochemical supercapacitor electrodes. *Scientific reports*, *9*(1), p.16315. https://doi.org/10.1038/s41598-019-52006-x.
14. Teo, E.Y.L., Muniandy, L., Ng, E.P., Adam, F., Mohamed, A.R., Jose, R. and Chong, K.F., 2016. High surface area activated carbon from rice husk as a high performance supercapacitor electrode. *Electrochimica Acta*, *192*, pp.110-119. https://doi.org/10.1016/j.electacta.2016.01.140.
15. Tewari, C., Pathak, M., Tatrari, G., Kumar, S., Dhali, S., Saha, B., Mukhopadhyay, P., Jung, Y.C. and Sahoo, N.G., 2024. Waste plastics derived reduced graphene oxide-based nanocomposite with Fe3O4 for water purification and supercapacitor applications. *Journal of Industrial and*

Engineering Chemistry, *130*, pp.346-356. https://doi.org/10.1016/j.jiec.2023.09.038.

16. Tatrari, G., Tewari, C., Karakoti, M., Pathak, M., Jangra, R., Santhibhushan, B., Mahendia, S. and Sahoo, N.G., 2021. Mass production of metal-doped graphene from the agriculture waste of Quercus ilex leaves for supercapacitors: inclusive DFT study. *RSC advances*, *11*(18), pp.10891-10901. 10.1039/D0RA09393A.
17. Tatrari, G., Tewari, C., Pathak, M., Karakoti, M., Bohra, B.S., Pandey, S., SanthiBhushan, B., Srivastava, A., Rana, S. and Sahoo, N.G., 2022. Bulk production of zinc doped reduced graphene oxide from tire waste for supercapacitor application: Computation and experimental analysis. *Journal of Energy Storage*, *53*, p.105098. 10.1016/j.est.2022.105098.
18. Khandelwal, M., Van Tran, C., Lee, J. and In, J.B., 2022. Nitrogen and boron co-doped densified laser-induced graphene for supercapacitor applications. *Chemical Engineering Journal*, *428*, p.131119. 10.1016/j.cej.2021.131119.
19. Wang, P., He, H., Xu, X. and Jin, Y., 2014. Significantly enhancing supercapacitive performance of nitrogen-doped graphene nanosheet electrodes by phosphoric acid activation. *ACS Applied Materials & Interfaces*, *6*(3), pp.1563-1568. https://doi.org/10.1021/am404277j.
20. Rawat, K.S., Tewari, C., Arya, T., Kim, Y.N., Pant, P., Sati, S., Dhali, S., Negi, P.B., Jung, Y.C. and Sahoo, N.G., 2025. Development of nitrogen and phosphorus dual-doped reduced graphene oxide from waste plastic for supercapacitor applications: Comparative electrochemical performance in different electrolytes. *Next Energy*, *6*, p.100209. https://doi.org/10.1016/j.nxener.2024.100209.
21. Abioye, A.M., Noorden, Z.A. and Ani, F.N., 2017. Synthesis and characterizations of electroless oil palm shell based-activated carbon/nickel oxide nanocomposite electrodes for supercapacitor applications. *Electrochimica Acta*, *225*, pp.493-502. https://doi.org/10.1016/j.electacta.2016.12.101.
22. Gajewska, K., Moyseowicz, A., Minta, D. and Gryglewicz, G., 2023. Effect of electrolyte and carbon material on the electrochemical performance of high-

voltage aqueous symmetric supercapacitors. *Journal of Materials Science*, *58*(4), pp.1721-1738.

23. Le Fevre, L.W., Cao, J., Kinloch, I.A., Forsyth, A.J. and Dryfe, R.A., 2019. Systematic comparison of graphene materials for supercapacitor electrodes. ChemistryOpen, 8(4), pp.418-428. https://doi.org/10.1002/open.201900004
24. Lee, J.H., Park, N., Kim, B.G., Jung, D.S., Im, K., Hur, J. and Choi, J.W., 2013. Restacking-inhibited 3D reduced graphene oxide for high performance supercapacitor electrodes. ACS nano, 7(10), pp.9366-9374. https://doi.org/10.1021/nn4040734
25. Zheng, S., Zhang, J., Deng, H., Du, Y. and Shi, X., 2021. Chitin derived nitrogen-doped porous carbons with ultrahigh specific surface area and tailored hierarchical porosity for high performance supercapacitors. *Journal of Bioresources and Bioproducts*, *6*(2), pp.142-151.
26. Bandara, T.M.W.J., Alahakoon, A.M.B.S., Mellander, B.E. and Albinsson, I., 2024. Activated carbon synthesized from Jack wood biochar for high performing biomass derived composite double layer supercapacitors. *Carbon Trends*, *15*, p.100359.
27. Jrad, E.B.H., Elmouwahidi, A., García, E.B., Marín, F.C. and Dridi, C., 2025. Biosynthetized activated carbon for sustainable supercapacitors development using aqueous and solid state electrolytes. *Journal of Power Sources*, *654*, p.237871.
28. He, M., Fic, K., Fra, E., Novák, P. and Berg, E.J., 2016. Ageing phenomena in high-voltage aqueous supercapacitors investigated by in situ gas analysis. *Energy & Environmental Science*, *9*(2), pp.623-633.
29. An, N., An, Y., Hu, Z., Guo, B., Yang, Y. and Lei, Z., 2015. Graphene hydrogels non-covalently functionalized with alizarin: an ideal electrode material for symmetric supercapacitors. *Journal of Materials Chemistry A*, *3*(44), pp.22239-22246.
30. Xu, Y., Lin, Z., Huang, X., Liu, Y., Huang, Y. and Duan, X., 2013. Flexible solid-state supercapacitors based on three-dimensional graphene hydrogel films. *ACS nano*, *7*(5), pp.4042-4049.
31. Bello, A., Barzegar, F., Momodu, D., Dangbegnon, J., Taghizadeh, F. and Manyala, N., 2015. Symmetric supercapacitors based on porous 3D interconnected carbon framework. *Electrochimica Acta*, *151*, pp.386-392.

32. Lai, C.C., Hsu, F.H., Hsu, S.Y., Deng, M.J., Lu, K.T. and Chen, J.M., 2021. 1.8 V Aqueous symmetric carbon-based supercapacitors with agarose-bound activated carbons in an acidic electrolyte. *Nanomaterials*, *11*(7), p.1731.
33. Ramasamy, C., Del Val, J.P. and Anderson, M., 2014. An analysis of ethylene glycol-aqueous based electrolyte system for supercapacitor applications. *Journal of Power Sources*, *248*, pp.370-377.
34. Liang, N., Ji, Y., Xu, J., Zuo, D., Chen, D. and Zhang, H., 2019. An asymmetric electric double-layer capacitor with a janus membrane and two different aqueous electrolytes. *Journal of Power Sources*, *423*, pp.68-71.
35. Karnan, M., Subramani, K., Sudhan, N., Ilayaraja, N. and Sathish, M., 2016. Aloe vera derived activated high-surface-area carbon for flexible and high-energy supercapacitors. *ACS applied materials & interfaces*, *8*(51), pp.35191-35202.
36. Cheng, Y., Huang, L., Xiao, X., Yao, B., Yuan, L., Li, T., Hu, Z., Wang, B., Wan, J. and Zhou, J., 2015. Flexible and cross-linked N-doped carbon nanofiber network for high performance freestanding supercapacitor electrode. *Nano energy*, *15*, pp.66-74.
37. Mun, Y., Jo, C., Hyeon, T., Lee, J., Ha, K.S., Jun, K.W., Lee, S.H., Hong, S.W., Lee, H.I., Yoon, S. and Lee, J., 2013. Simple synthesis of hierarchically structured partially graphitized carbon by emulsion/block-copolymer co-template method for high power supercapacitors. *Carbon*, *64*, pp.391-402.
38. Wei, T., Wei, X., Gao, Y. and Li, H., 2015. Large scale production of biomass-derived nitrogen-doped porous carbon materials for supercapacitors. Electrochimica Acta, 169, pp.186-194.
39. Guo, C., Li, N., Ji, L., Li, Y., Yang, X., Lu, Y. and Tu, Y., 2014. N-and O-doped carbonaceous nanotubes from polypyrrole for potential application in high-performance capacitance. Journal of Power Sources, 247, pp.660-666.
40. Uniyal, D., Karakoti, M., Morávková, Z., Konefał, M., Lhotka, M., Hromádková, J., Jarek, M. and Bober, P., 2026. Surface-engineered porous carbon electrode with polyaniline for high-energy density symmetric and Zn-ion hybrid supercapacitor. Journal of Energy Storage, 152, p.120561.
41. Parida, S., Sahu, K.C., Sahoo, B.B., Pandey, V.S., Thatoi, D.N., Nayak, N. and Nayak, M.K., 2023. High performance supercapacitor electrodes from automobile

soots: An effective approach to control environmental pollution. Inorganic Chemistry Communications, 158, p.111671.

42. Wu, C.Y., Chang, C.Y., Tsai, S.W., Lin, S.C., Hsu, T.C. and Hsieh, T.H., 2024. Activated carbon for supercapacitor electrodes produced by the carbonation and activation of glucose with potassium nitrate. ACS Applied Energy Materials, 7(16), pp.6873-6886.
43. Ahmad, N., Rinaldi, A., Sidoli, M., Magnani, G., Morenghi, A., Scaravonati, S., Vezzoni, V., Pasetti, L., Fornasini, L., Ridi, F. and Milanese, C., 2024. High performance quasi-solid-state supercapacitor based on activated carbon derived from asparagus waste. Journal of Energy Storage, 99, p.113267.
44. Gao, Y., Huynh, N.T., Kim, K.J., Wang, C., Pham, V.H. and Matranga, C., 2024. Upcycling linear low-density polyethylene waste to turbostratic graphene for high mass loading supercapacitors. Chemical Engineering Journal, 498, p.155873.
45. Rawat, K.S., Tewari, C., Arya, T., Pant, P., Kim, Y.N., Kumar, R., Jung, Y.C. and Sahoo, N.G., 2026. Sustainable conversion of waste plastic into reduced graphene oxide for superior supercapacitor applications: A comparative electrolyte study. Journal of Power Sources, 661, p.238601.
46. Bhatt, D., Kokulnathan, T., Wang, T.J., Sahoo, N.G., Ahmed, F. and Alshahrani, T., 2026. Synergistic construction of ZIF-67 MOF-derived trimetallic NiCoFe-LDH anchored on reduced graphene oxide from waste tires for high-retention supercapacitors. Journal of Power Sources, 673, p.239656.
47. Bhatt, D., Kokulnathan, T., Wang, T.J., Ghanem, M.A. and Sahoo, N.G., 2025. Powering sustainability: High-performance supercapacitors using reduced graphene oxide from waste tires embedded with molybdenum disulfide. Journal of Power Sources, 642, p.236932.